Bulk temperature mapping of broad area quantum dot lasers: modeling and micro-thermographic analysis

Jayanta Mukherjee[1*], Mathias Ziegler[2], Julien LeClech[2], Jens W. Tomm[2*],
Brian Corbett[1], John G. Mclnerney[1], Johann Peter Reithmaier[3], S. Deubert[4] and A. Forchel[4]
[1]Dept of Physics and Tyndall National Institute, University College, Cork, Ireland
[2]Max-Born-Institut, Max-Born-Str. 2 A, 12489 Berlin, Germany
[3]Institute of Nanostructure Technologies and Analytics, Technische Physik, Universität Kassel, Heinrich-Plett-Str. 40, 34132 Kassel, Germany
[4]Technische Physik, Universität Würzburg, Am Hubland, 97078 Würzburg

ABSTRACT

For novel devices such as quantum dot lasers, the usual thermal characterization using temperature induced wavelength shift is ineffective due to weak thermal shift of the inhomogeneously broadened gain-peak. This calls for new thermal characterization techniques for such devices. To this end we have analyzed bulk thermal properties of broad area quantum dot lasers theoretically, and have experimentally verified these calculations using the novel technique of micro-thermography. InGaAs/GaAs 950 nm emitting, 50 µm wide and 1.5 mm long, large optical cavity quantum dot lasers were used for the study. Our two-dimensional steady-state model self-consistently includes current spreading and distributed heat sources in the device and using finite element method reproduces high resolution temperature maps in the transverse cross section of the diode laser. A HgCdTe based thermocamera with detection spectral range 3.5-6.0 µm was employed for micro-thermography measurements. Its microscope with 6x magnification has a nominal spatial resolution of 4 µm/pixel for full frame images of 384×288 pixels. A ray tracing technique was used to model the propagation of thermal radiation inside the transparent laser die which in turn links calculated and experimentally derived temperature distributions. Excellent agreement was achieved which verifies the model-calculation and the thermal radiation propagation scheme inherent in the experimental approach. This result provides a novel means for determining reliable bulk temperature data from quantum dot lasers.
Keywords: Quantum dot, thermal model, FEM, Thermography.

1. INTRODUCTION

Not long after the first theories of quantum dot (QD) lasers were outlined, it was realized that these devices have great potential for high power and high brightness applications[1]. Along with low threshold current densities, broad spectral gain profiles and inhibited in-plane carrier diffusion, quantum dot lasers are expected to have reduced values of phase-amplitude coupling (or alpha) parameter[1], which drives self-focusing in the media. While the low lasing threshold and reduced in-plane carrier diffusion raises the facet damage threshold under high power operation, weak phase-amplitude coupling helps in suppressing filamentation thereby increasing spatial coherence (brightness) of the output beam. While semiconductor laser designs based on QD active region continue to improve and deliver high power with enhanced brightness, thermal management issues which have prevented extraction of useful power from diode lasers and beleaguered their reliability still remains a challenge. Systematic investigation of thermal properties in semiconductor lasers is of extreme importance as it not only affects the gain medium but also influences the modal behavior and stability, especially for devices designed for high brightness output[2]. For QD lasers this is a very challenging task, both experimentally and from the theoretical modeling point of view. While the reduced temperature sensitivity of emission wavelength in devices with QD active medium renders the standard experimental method of junction temperature assessment ineffective[3], the stiff aspect ratios encountered in the epitaxial design of these devices make accurate numerical modeling an extremely difficult task[2]. In this paper we report a systematic analysis of the bulk thermal properties of broad area QD lasers. We use a self-consistent electro-thermal model to theoretically calculate tem-

*j.mukherjee@ucc.ie

Novel In-Plane Semiconductor Lasers VIII, edited by Alexey A. Belyanin, Peter M. Smowton,
Proc. of SPIE Vol. 7230, 72300W · © 2009 SPIE · CCC code: 0277-786X/09/$18 · doi: 10.1117/12.808298

perature maps in the device and then verify the model-calculations experimentally using the novel technique of micro-thermography (MT)[4]. The two-dimensional (2-D) electro-thermal model is designed and simulated using finite element method (FEM)[2], temperature maps from which are then processed via a ray-tracing technique to mimic the light propagation effect inherent in MT[5] and the obtained infrared images are compared with experimental results. Excellent agreement obtained between theoretical and experimental results establishes the effectiveness of MT as a future experimental probe for microscopic thermal analysis of not only quantum dot lasers but semiconductor devices in general.

2. THEORETICAL MODEL

The 950 nm emitting broad area (BA) QD lasers used in our analysis are based on a large optical spot size design with a 2.5µm thick $Al_{0.3}Ga_{0.7}As$ core region. Three layers of highly strained $In_{0.53}Ga_{0.47}As$ QD's are spaced within 30 nm of GaAs spacer layers. The structure is grown by molecular beam epitaxy on GaAs substrates. Photoluminescence measurement show that the ground state is at 934 nm and the first excited state is at 901 nm. 50-µm-wide silicon dioxide isolated stripe lasers were fabricated using TiPtAu as the p-side contact metallization. Samples were thinned to approximately 100 µm and AuGeNi metallization was used as the n-contact. Devices of various lengths were analyzed. The 1.5 mm long p-side down packaged device had a threshold current of 0.45 A, with total slope efficiency of 0.72 W/A, and lasing wavelength at 950 nm. While a total of 4 devices were analyzed, we confine the presentation here to one device. The device under consideration has its contact stripe asymmetrically placed on the 500 µm wide device. The stripe center is located at 185 µm from one side. The lasing threshold for this device is 0.4 A and the output power at 2 A of operation current is about 0.55 W.

We apply a 2D steady-state electro-thermal FEM model and do not consider facet heating. This is justified as we are interested in bulk thermal properties of the laser. Temperature profile and current spreading in the device was simulated using a model developed in our earlier work[2]. No current spreading was assumed in the substrate on account of high mobility of electrons. In addition to joule heating, distributed heat sources taken into account in the model include re-absorption of stimulated and spontaneous emission as well as non-radiative recombination. Epitaxial structure dependent radiative transfer heating is not involved in the laser structure under analysis and hence is not considered in the model. Heat transfer via convection and radiation was also not included in the final model as it was found to be of little effect. 2D heat-conduction equation coupled with Laplace's equation was self-consistently solved in the steady state using FEM in a 2D lateral cross section[2]. A flux-less Neumann boundary (thermal insulation) is assumed at all the laser air interfaces and a Dirichlet boundary is assumed at the In-solder Cu-heat sink interface. The Dirichlet boundary (equal to ambient temperature) assumes that the Cu-heat sink is of infinite thermal conductivity. We believe that this usual assumption[6], might affect the actual magnitude of the temperature but will not affect its lateral profile. Both asymmetric and symmetric device were simulated to quantify the effect of asymmetry on temperature profile.

Since semiconductor materials are semitransparent in the mid-infrared[7], intra-cavity propagation of thermal radiation which results in an effective broadening of the MT thermal images must be taken into account while comparing theoretical and experimental results. This is achieved using a ray-tracing technique. The calculations are performed using commercially available ZEMAX® software[8]. The device geometry is modeled as two homogeneous cuboids, a 100 µm-thick one for the GaAs substrate and a 4 µm-thick one for the epi-layer region, with refractive indices of 3.3 and 3.0, respectively, and absorption coefficients of 12 cm^{-1}. While the four semiconductor-air interfaces are uncoated, a reflectivity of 1 is assumed for the top and bottom surfaces (p- and n-contact metallization). The detection plane of the software is placed at a position in front of the device, where in reality the MT system is located. Temperature distributions given by FEM are transformed into sources of spatially isotropic and unpolarized thermal radiation and are placed accordingly in the ray-tracing model[5]. Starting point are the 2D FEM temperature distributions that are homogeneously extended into the bulk along the laser axis. In Figs. 1 (a) and (d) FEM maps are displayed with a spatial resolution that already corresponds to the pixel size of our MT system in the vertical direction, whereas horizontally a 10 µm grid was chosen. By using the reverse temperature calibration, this data provides a 3D distribution of the thermal radiation sources (in units of camera counts). The MT-image formation is then simulated by ray-tracing the thermal radiation towards the camera and a subsequent temperature re-calibration [Figs. 1 (b), (e)]. Such processed FEM data and the experimental data [Figs. 1 (c), (f)] can already be compared qualitatively.

3. MICRO-THERMOGRAPHIC ANALYSIS

Conventional thermography has been applied in order to probe, in a rather qualitative way, information about temperatures in double-heterostructure lasers,[9-11] quantum-well lasers,[12,13] light-emitting diodes,[14] high-power diode laser arrays,[15] and even stacked two-dimensional laser arrays.[16] The capability to probe static temperature distributions, determined through the front facet of high-power broad-area lasers and laser arrays,[4,5,17-22] along with the ability to quantify the transient temperature evolution of active regions and device packages,[23-26] made thermography a convenient tool for device characterization and considerably improved the understanding of important degradation mechanisms in such devices.[18,19,21,24,26] Such measurements of quantum-well devices involved determination of absolute temperatures from the thermographic data up to high spatial resolutions (i.e., micro-thermography). Thus MT is prepared to be applied to QD-lasers, where a reference probe for the temperature is missing.

Our experimental MT analysis employed a THERMOSENSORIK CMT 384M system with a detection range confined to the 3.5-6.0 µm. The HgCdTe camera microscope with six-fold magnification delivers a nominal spatial resolution of 4 µm/pixel for full frame images of 384×288 pixel, but almost diffraction limited to about 7 µm. The calibration is made by taking images between 25 and 35 °C in 2°C steps. The corresponding temperature vs. camera signal curve is perfectly described by a third order polynomial. Temperature-calibrated images obtained in this way are presented in Figs. 1 (c) and (f) for operation currents of 0.9 and 1.8 A, respectively.

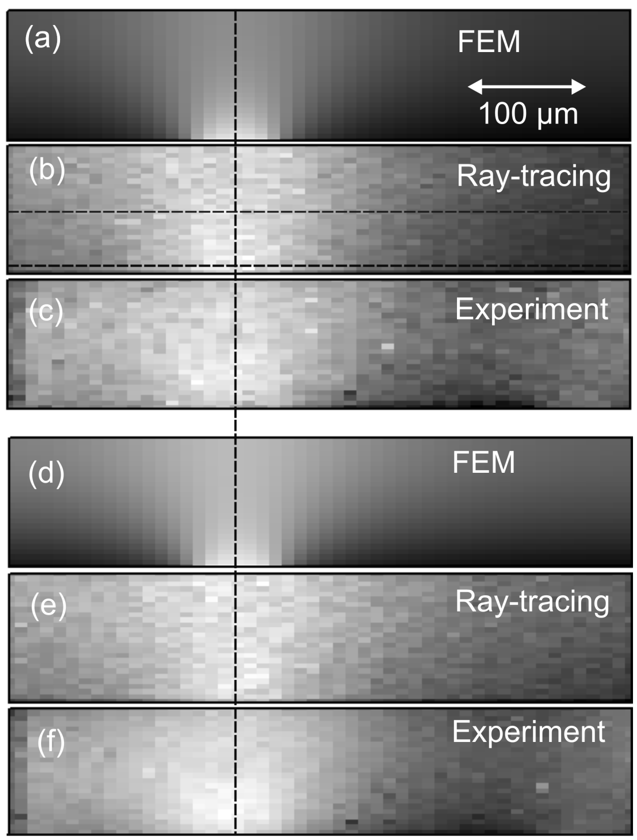

Fig. 1. Modeled and measured normalized thermographic images from a QD-laser operated at 0.9 (a-c) and 1.8 A (d-f). (a) and (d) represent temperature distributions obtained by 2D-FEM thermal simulation, (b) and (e) additionally involve the smearing effect due to the propagation of thermal radiation within the device as modeled by ray-tracing. The dashed lines mark the locations, where the cuts that are discussed in the following figures are taken.

4. RESULTS

In order to compare FEM simulated temperature maps, which we consider to represent the true thermal distribution in the device, with MT data, we use the ray-tracing transformed FEM maps which give maps of infrared radiation as seen by the infrared camera. Propagation of intra-cavity thermal radiation considerably broadens the FEM temperature maps resulting in a close agreement with the experimental maps.

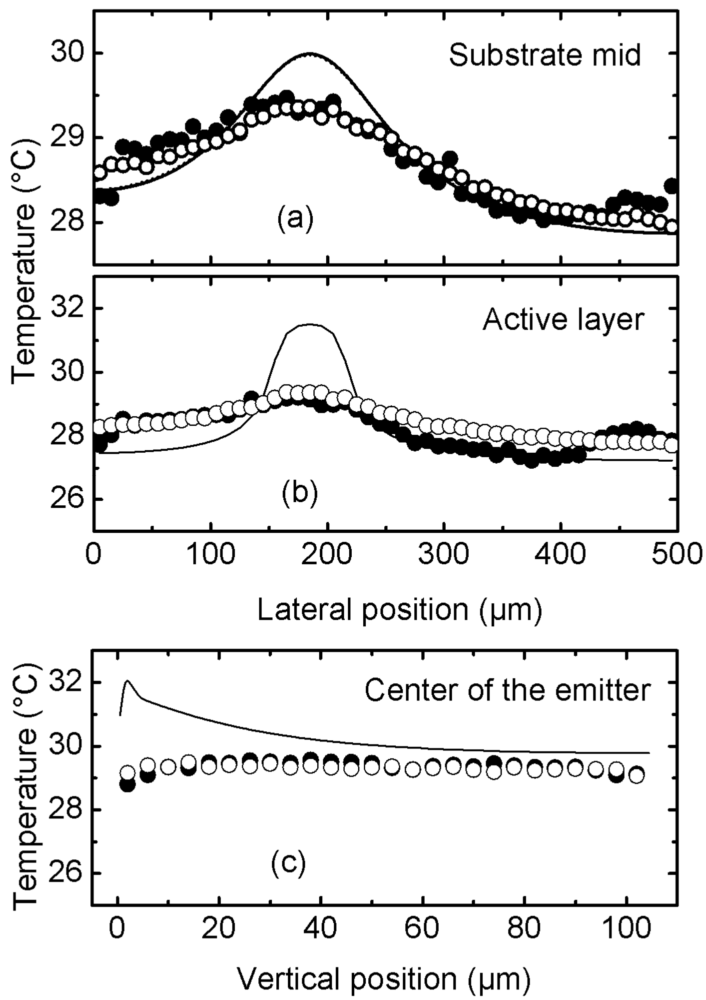

Fig. 2. Absolute temperature profiles from a QD-laser operated at 0.9 A obtained as cuts from the maps given in Fig. 1(a) (lines), 1(b) (open circles), and 1(c) (closed circles). (a) Lateral profiles around the active layer. (b) Lateral profiles around half the device heights. (c) Vertical profiles around the stripe centre. All profiles are averaged from three pixel rows or columns for noise reduction.

The quantitative comparison is based on cuts through these maps; see dashed lines in Fig. 1. In Figs. 2 and 3 the FEM data (lines), FEM data after the above described processing (open circles), and the data as obtained from MT experiment (full circles) are compared for two operation currents of 0.9 A (Fig. 2) and 1.8 A (Fig. 3) in terms of lateral (along active layer and middle of the device) and vertical cuts (emitter centre, along growth direction). In all cases, there is an exceptionally good agreement between the open and full circles. The only adjustment parameter in this comparison is the heat-sink temperature. The FEM model assumes a fixed temperature of 25.0 °C at the device heat-sink interface, whereas in the experiment the heat-sink temperature was controlled to 25.0±0.2 °C approximately 4 mm away, which could result in a small relative temperature difference. In order to nearly perfectly match model and experiment, heat-sink temperatures of 26.1 °C [0.9 A, (Fig. 2)] and 25.0 °C [1.8 A, (Fig. 3)] are assumed. In turn, such close agreement strongly indicates that not only propagation of thermal radiation within the cavity is a key issue towards quantitative MT analysis on a microscopic scale, also the 2D - FEM model is sufficient to reproduce the experimental results.

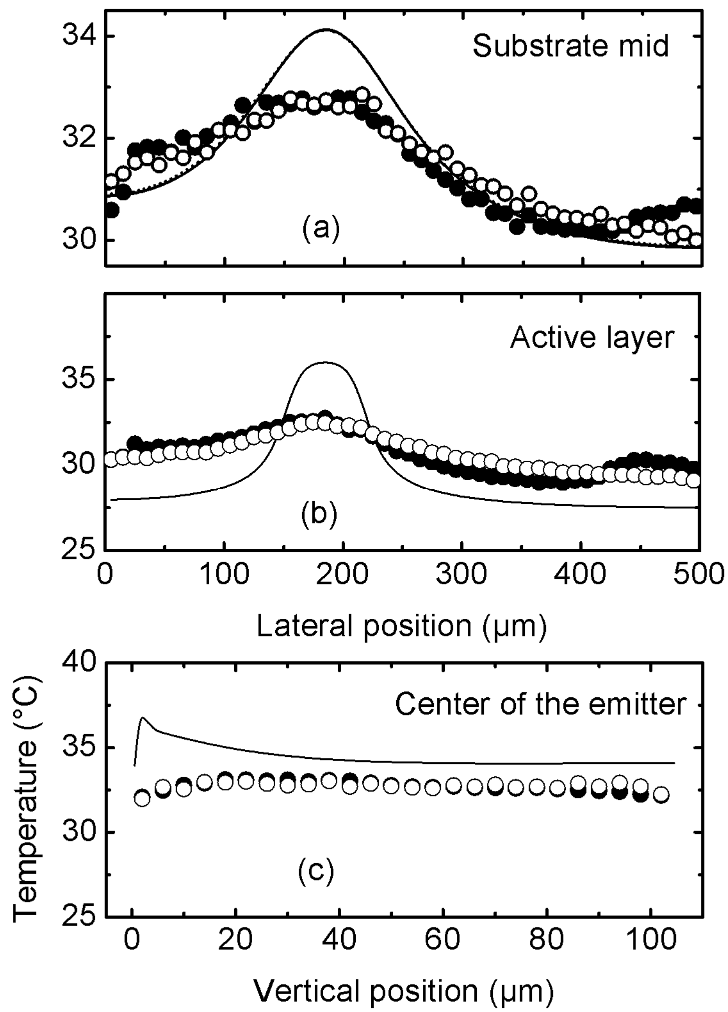

Fig. 3. Absolute temperature profiles from a QD-laser operated at 1.8 A obtained as cuts from the maps given in Fig. 1(d) (lines), 1(e) (open circles), and 1(f) (closed circles). The given profiles are analogous to Fig. 2.

In summary, we have analyzed steady-state bulk thermal properties of QD-lasers both theoretically and experimentally. This is particularly important because for diode laser with QD active medium, use of the emission wavelength shift as method for thermal analysis widely fails. In order to directly compare the experimental results with FEM calculations, propagation of thermal radiation through the device must be taken into account. This is accomplished by a ray-tracing model. The close agreement between MT and modeling in terms of shape and magnitude verifies both the used thermal radiation propagation scheme that is inherent to the thermographic approach and the FEM model in addition to the usefulness of MT. Thus, we established a methodology to extract reliable bulk temperature data for QD lasers on a microscopic scale.

ACKNOWLEDGEMENTS

The study was funded by the European Commission within the project WWW.BRIGHTER.EU, Contract no. 035 266.

REFERENCES

[1] D. Bimberg, M. Grundmann, N. N. Ledentsov, Quantum Dot Heterostructures, John Wiley & Sons, Chichester, UK (1999).

[2] J. Mukherjee and J. McInerney, "Electrothermal analysis of CW high-power broad-area laser diodes: A comparison between 2-D and 3-D modeling," IEEE J. Select. Top. Quantum Electron. 13 (5), 1180 (2007).

[3] F. Klopf, S. Deubert, J. P. Reithmaier, and A. Forchel, "Correlation between the gain profile and the temperature-induced shift in wavelength of quantum-dot lasers," Appl. Phys. Lett. 81, 217 (2002).

[4] A. Kozlowska, M. Latoszek, Jens W. Tomm, F. Weik, T. Elsaesser, M. Zbroszczyk, M. Bugajski, B. Spellenberg, and M. Bassler, "Analysis of thermal images from diode lasers: Temperature profiling and reliability screening," *Appl. Phys. Lett.*, 86(20), 203503 (2005).

[5] J. LeClech, M. Ziegler, J. Mukherjee, J. W. Tomm, T. Elsaesser, J.-P. Landesman, B. Corbett, J. G. Mclnerney, J. P. Reithmaier, S. Deubert, A. Forchel, W. Nakwaski, and R. P. Sarzała, "Micro-thermography of diode lasers: the impact of light propagation on image formation," J. Appl. Phys., In print, (2008).

[6] W. Nakwaski, Int. J. Optoelectron. 5, 451 (1990).

[7] M. Ziegler, J. W. Tomm, T. Elsaesser, C. Monte, J. Hollandt, H. Kissel, and J. Biesenbach, "Cavity-enhanced thermal emission from semiconductor lasers," J. Appl. Phys., 103(10), 104508 (2008).

[8] www.zemax.com

[9] T. Kobayashi, T. Kawakami, and Y. Furukawa, "Thermal diagnosis of dark lines in degraded GaAs-AlGaAs double-heterostructure lasers," *Jpn. J. Appl. Phys.*, 14(4), 508 (1975).

[10] T. Kobayashi, Y. Seki, and Y. Furukawa, "Optical absorption at dark lines in degraded double-heterostructure lasers," *Jpn. J. Appl. Phys.*, 14(4), 516 (1975).

[11] T. Kobayashi and Y. Furukawa, "Temperature distributions in the GaAs-AlGaAs double-heterostructure laser below and above threshold current," *Jpn. J. Appl. Phys.*, 14(12), 1981 (1975).

[12] M. Passlack, C. G. Bethea, W. S. Hobson, John Lopata, E. F. Schubert, G. J. Zydzik, D. T. Nichols, J. F. de Jong, U. K. Chakrabarti, and N. K. Dutta, "Infrared microscopy studies on high-power InGaAs-GaAs-InGaP lasers with Ga_2O_3 facet coatings," *IEEE J. Sel. Top. Quant .Elec.*, 1(2), 110 (1995).

[13] W. Fang, C. G. Bethea, Y. K. Chen, and S. L. Chuang, "Longitudinal spatial inhomogeneities in high-power semiconductor lasers," *IEEE J. Sel. Top. Quant. Elec.*, 1(2), 117 (1995).

[14] V. K. Malyutenko, "Mapping of current and heat flows in IR light emitting devices and lasers," *Proc. SPIE*, 4648 (1), 43 (2002).

[15] J. Troger, M. Schwarz, and A. Jakubowicz, "Measurement systems for the investigation of soldering quality in high-power diode laser bars," *J. Lightwave Techn.*, 23(11), 3889, (2005).

[16] B. L. Meadows, F. Amzajerdian, N. R. Baker, V. Sudesh, and U. N. Singh et al. , "Thermal characteristics of high-power, long pulse width, quasi-cw laser diode arrays," *Proc. SPIE*, 5336(1), 203 (2004).

[17] A. Kozlowska, P.Wawrzyniak, J. W. Tomm, F.Weik, and T. Elsaesser, "Deep level emission from high-power diode laser bars detected by multispectral infrared imaging," *Appl. Phys. Lett.*, 87,153503 (2005).

[18] A. Kozlowska, P.Wawrzyniak, A. Malag, M. Teodorczyk, J. W. Tomm, and F. Weik, "Reliability screening of diode lasers by multispectral infrared imaging," *J. Appl. Phys.*, 99(5), 053101 (2006).

[19] J. W. Tomm, T. Q. Tien, M. Ziegler, F. Weik, B. Sumpf, M. Zorn, U. Zeimer, and G. Erbert, "Degradation behavior and thermal properties of red (650 nm) high-power diode single emitters and laser bars," *Proc. SPIE*, 6456(1), 645606 (2007).

[20] M. Ziegler, J. W. Tomm, F. Weik, T. Elsaesser, C. Monte, J. Hollandt, H. Kissel, G. Seibold, and J. Biesenbach, "Accurate determination of absolute temperatures of GaAs based high-power diode lasers," *Proc. SPIE*, 6876, 68761A (2008).

[21] J. W. Tomm, M. Ziegler, T. Q. Tien, F. Weik, P. Hennig, J. Meusel, H. Kissel, G. Seibold, J. Biesenbach, G. Groenninger, G. Herrmann, and U. Strauß, "Screening of high power laser diode bars in terms of stresses and thermal profiles," *Proc. SPIE*, 6876, 687619 (2008).

[22] D. Pierscinska, A. Kozlowska, K. Pierscinski, M. Bugajski, J. W. Tomm, M. Ziegler, and F. Weik, "Thermal processes in high-power laser bars investigated by spatially resolved thermoreflectance," *J. Mater. Sci.*, 19, S150 (2008).

[23] M. Ziegler, F.Weik, J. W. Tomm, T. Elsaesser, W. Nakwaski, R. P. Sarzała, D. Lorenzen, J. Meusel, and A. Kozlowska, "Transient thermal properties of high-power diode laser bars," Appl. Phys. Lett., 89(26), 263506 (2006).

[24] M. Ziegler, J. W. Tomm, T. Elsaesser, C. Matthiesen, M. Bou Sanayeh, and P. Brick, "Real-time thermal imaging of catastrophic optical damage in red-emitting high-power diode lasers," *Appl. Phys. Lett.*, 92(10), 103514 (2008).
[25] M. Ziegler, J. W. Tomm, T. Elsaesser, G. Erbert, F. Bugge, W. Nakwaski, and Robert P. Sarzała, "Visualization of heat flows in high-power diode lasers by lock-in thermography," *Appl. Phys. Lett.*, 92(10), 103513 (2008).
[26] M. Bou Sanayeh, P. Brick, W. Schmid, B. Mayer, M. Müller, M. Reufer, K. Streubel, M. Ziegler, J. W. Tomm, and G. Bacher, "The physics of catastrophic optical damage in high-power AlGaInP laser diodes," *Proc. SPIE*, 6997, 699703 (2008).